

A quantitative evaluation of the role of the Argentinean Col and the Low Pressure Tongue East of the Andes for frontogenesis in the South American subtropics

H. M. J. Barbosa¹ and J. M. Arraut²

¹Instituto de Física, Universidade de São Paulo, Rua do Matão, 187, São Paulo SP 05508-090, Brazil

²Centro de Ciências do Sistema Terrestre, Instituto Nacional de Pesquisa Espaciais, Av. dos Astronautas, 10758, São José dos Campos SP 12227-000, Brazil

Received: 26 April 2009 – Revised: 12 June 2009 – Accepted: 17 June 2009 – Published: 13 October 2009

Abstract. Previous studies have found the South American subtropics to exhibit high climatological frontogenesis in equivalent potential temperature during the austral summer. An important contribution to this pattern is given by frontogenesis over the Argentinean Col (AC), which separates the Northwestern Argentinean Low (NAL) from transient troughs to the south of it. The NAL and the Low Pressure Tongue east of the Andes (LPT) promote efficient transport of Amazonian humidity to the subtropics during the incursion of transient disturbances over the continent. The convergence of this strong warm and humid flow with mid-latitude air brought into the subtropics by the disturbance occurs preferentially in the neighborhood of the AC. The main difficulty in quantifying the contribution of the NAL, AC and LPT structure to frontogenesis in the South American subtropics is the automatic detection of the AC and LPT. In this paper an algorithm developed to this end is briefly presented and applied to obtain statistics on the role of these structures in frontogenesis. Six-hourly data from ECMWF ERA-40 Reanalysis over 21 austral summer periods (December–March) is used. Occurrences of the AC are highly concentrated between 34–39° S and 66–69° W, being present in this region in 42% of the time instants analyzed. The spatial average of the positive values of the frontogenesis over this region was calculated for each time step as a measure of intensity and histograms were built for the cases when the AC was and was not found inside this region. Mean, median and mode are larger for the distribution of cases with the presence of the AC. In addition, we present the frequency of occurrence of the AC as a function of the frontogenesis, showing that

it grows with the intensity of the frontogenesis, rising above the 0.955 quantile. We have not found any correlation between the AC frequency and the frontolysis intensity.

1 Introduction

South American subtropics exhibit high climatological frontogenesis in equivalent potential temperature during summer and deformation of the wind field is the main contributing mechanism. An analysis of the synoptic conditions present in high frontogenesis situations revealed the presence of the Northwestern Argentinean Low (NAL) and a transient trough to its south, both surrounded by an elongated trough, which has been named the Low Pressure Tongue east of the Andes (LPT). The neighborhood of the col separating the NAL from the transient trough to its south, named the Argentinean Col (AC), is a preferred spot for frontogenesis. The NAL and the LPT promote efficient transport of Amazonian humidity to the subtropics and mid-latitudes. The convergence of this strong warm and humid flow with mid-latitude air occurs preferentially in the neighborhood of the AC, which separates the NAL from the transient trough, making it very prone to frontogenesis (Arraut, 2007; Arraut and Barbosa, 2009).

An interesting question is to quantify the contribution of the NAL, AC and LPT structures to frontogenesis by deformation in the South American subtropics. However the main obstacle in doing so is the need for automatic detection of the AC and LPT. The goal of this paper is to present such a quantitative study, as well as the algorithm developed for automatic detection of these features of the geopotential field. It will be shown from a statistical view point that: (a) the presence of the AC and LPT favors frontogenesis, (b) the higher



Correspondence to: H. M. J. Barbosa
(hbarbosa@if.usp.br)

the frontogenesis the higher the statistical presence of these features, and (c) the AC and LPT are present in the majority of cases of high frontogenesis.

2 Data and Methods

Temperature, humidity and geopotential fields are taken from the European Centre for Medium Range Weather Forecasts (ECMWF) 40 years Reanalysis (ERA-40). Twenty one December to March seasons, from December 1981 to March 2002, are studied as in Arraut (2007). Equivalent potential temperature, θ_e , is calculated according to Bolton (1980). Frontogenesis in θ_e is calculated as a sum of four terms, following Ninomiya (1984):

$$FG = \frac{d|\nabla\theta_e|}{dt} = FG_1 + FG_2 + FG_3 + FG_4 \quad (1)$$

The four terms are:

$$FG_1 = \frac{1}{|\nabla\theta_e|} \left[(\nabla\theta_e \cdot \nabla) \frac{d\theta_e}{dt} \right] \quad (2)$$

$$FG_2 = -\frac{1}{2|\nabla\theta_e|} (\nabla\theta_e)^2 \left(\frac{\partial u}{\partial x} + \frac{\partial v}{\partial y} \right) \quad (3)$$

$$FG_3 = -\frac{1}{2|\nabla\theta_e|} \left[\left(\frac{\partial\theta_e}{\partial x} \right)^2 - \left(\frac{\partial\theta_e}{\partial y} \right)^2 \right] A + 2 \frac{\partial\theta_e}{\partial x} \frac{\partial\theta_e}{\partial y} B \quad (4)$$

$$FG_4 = -\frac{1}{|\nabla\theta_e|} \frac{\partial\theta_e}{\partial p} \left(\frac{\partial\theta_e}{\partial x} \frac{\partial w}{\partial x} + \frac{\partial\theta_e}{\partial y} \frac{\partial w}{\partial y} \right) \quad (5)$$

where u , v , w are the wind components and $A = \partial u / \partial x - \partial v / \partial y$ and $B = \partial v / \partial x + \partial u / \partial y$ are deformation terms. FG_1 is the frontogenesis due to diabatic changes of θ_e . FG_2 and FG_3 are associated with the large scale horizontal flow. The first represents the effect of divergence and the latter that of deformation. FG_4 accounts for vertical advection of θ_e . FG_3 was found to be the most important term in subtropical South America (Arraut and Barbosa, 2009). This is in accordance with Ninomiya (1984) and Kodama (1992) who found it to be the main contributor to frontogenesis in the troposphere.

Based on these data an algorithm was developed to automatically detect the NAL, AC and LPT and applied to 10 184 six hour intervals to obtain statistics on the role of these structures in frontogenesis in θ_e over the South Americas subtropics. This algorithm can be divided into three main blocks: (1) locate NAL by searching for minima of the 850 hPa geopotential field, ϕ_{850} , (2) locate AC by searching for minima of $\nabla\phi_{850}$ and (3) locate LPT by searching for a self connection of ϕ_{850} that passes through AC and contains the NAL.

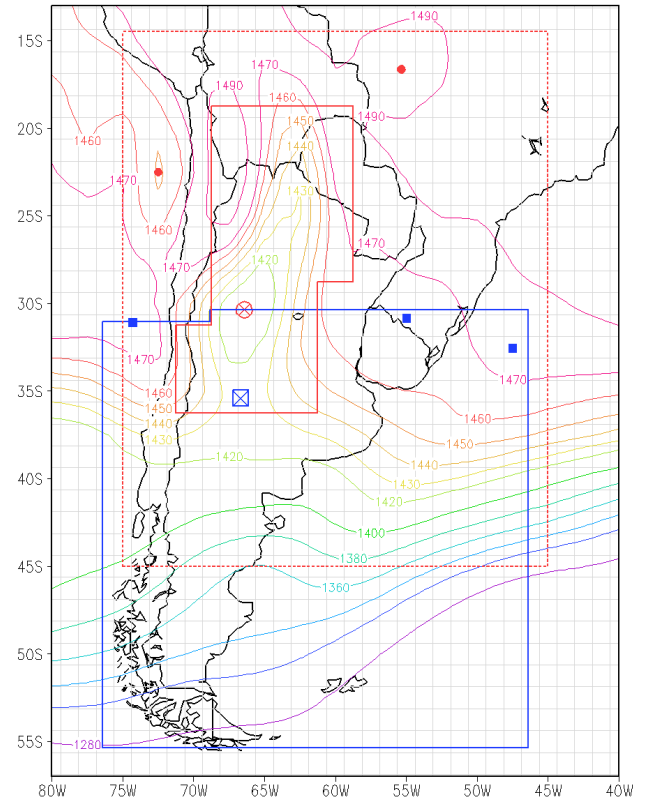


Fig. 1. Contours show ϕ_{850} (m) at 12 Z 24 December 1991. Polygons delimit search regions for: minimums of ϕ_{850} (dotted red); NAL position (red); AC position (blue). Markers indicate: lows (red), NAL (big red), cols (blue), AC (blue square)

2.1 Locate NAL

The first part of the algorithm detects the presence of the NAL, defined to be southernmost minimum of the 850 hPa geopotential field inside the region where the NAL is climatologically expected to be found, (full red line in Fig. 1).

Firstly a continuous geopotential function ϕ_{850} is defined, through the interpolation of the original $2.5^\circ \times 2.5^\circ$ gridded dataset. Then a search for local minima of ϕ_{850} (lat, lon) is performed using Powells minimization method in multi dimensions (Acton, 1990) as implemented by Press et al. (1992). Because numerical algorithms such as this will only search and find local minima close to the first guess, we take as candidate positions to the minimization algorithm the centers of all grid-points with values smaller than their neighbors. Figure 1 shows as a dotted red line the region used to select the initial positions from. To avoid convergence problems from the minimization algorithm, for all minima found it is verified if the laplacian of the geopotential field is greater than zero, $\nabla^2\phi_{850} = \partial^2\phi_{850}/\partial x^2 + \partial^2\phi_{850}/\partial y^2 > 0$, a necessary condition for a point to be a minimum. For the

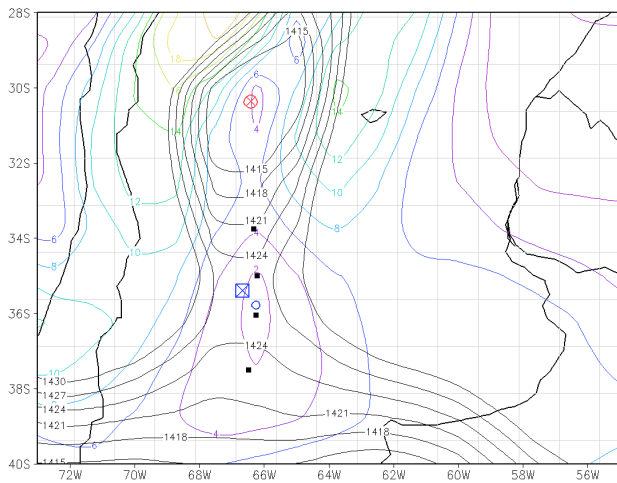


Fig. 2. Contours show the magnitude of $\nabla\phi_{850}$ (colors) and ϕ_{850} (black). Markers indicate: position of NAL (red circle), AC as candidate positions (black), position of AC as detected by the gradient (blue circle) and position of AC corrected using ϕ_{850} (blue square).

example situation presented in Fig. 1, the red markers show the minima found. From all of these, the southern most inside the climatological NAL region is taken to be the NAL.

2.2 Locate AC

If the Northwestern Argentinean Low is found at a given time, the algorithm searches for the col which separates the NAL from transient troughs to the south of it. Because AC is a mathematical saddle point of the geopotential field, it is also a minimum of the geopotential gradient. The algorithm takes advantage of this property for locating AC and basically repeats the procedure described above using the gradient instead of the field itself.

Firstly $|\nabla\phi_{850}|$ is calculated by finite differencing the original gridded dataset and then a continuous function is defined through its interpolation. Secondly, the minimization algorithm is used with initial positions taken to be the centers of the grid-points with values smaller than at least seven of their neighbors and the search is done only up to 25° to the south of the NAL (blue line in Fig. 1). This relaxed condition was found to be necessary because the finite differencing process can sometimes masks out true initial conditions. With this relaxation there are substantially more first guesses but all local minima of $|\nabla\phi_{850}|$ are guaranteed to be found. Figure 2 shows the geopotential field in colored contours, the initial trial positions (black) and the found minimum (blue circle) for the same example situation as in Fig. 1. In this case all initial positions converged to the same minimum.

Finally, the positions found might correspond to maximums or minimums of ϕ_{850} which are excluded by looking at ϕ_{850} in the point's neighborhood. The top panel Fig. 3

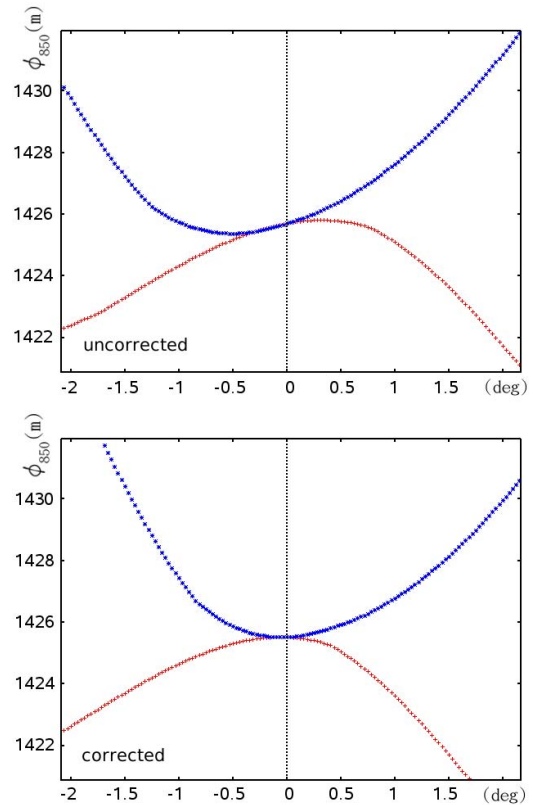


Fig. 3. The two panels show ϕ_{850} as a function of the distance (degrees) away from AC and along the directions of maximum growth (blue) and diminish (red) before (top) and after (bottom) the correction using ϕ_{850} is applied.

shows the geopotential as a function of the angular distance away from the tested point and along the perpendicular directions of its maximum (blue) and minimum (red) growth. In this particular case it is clear that the determinant of the Hessian matrix (i.e. the product of the curvatures) is negative and hence the point is indeed a saddle.

This graph also shows that the saddle position determined by minimizing $|\nabla\phi_{850}|$ is not exactly at the right place because the curves are not tangent at their inflection points. The algorithm then uses this information to move the point around until it finds the correct position, as shown in the lower panel of Fig. 3. The uncorrected and corrected positions are shown in Fig. 2 as a blue circle and a blue square respectively. A comparison with the geopotential shown in black contour shows the correction to be indeed necessary.

2.3 Locate the Tongue

If any cols were found, the algorithm follows on to verify which one is associated with the NAL. Because the Argentinean Col separates the NAL from transient troughs to the south of it and the AC is a mathematical saddle point of

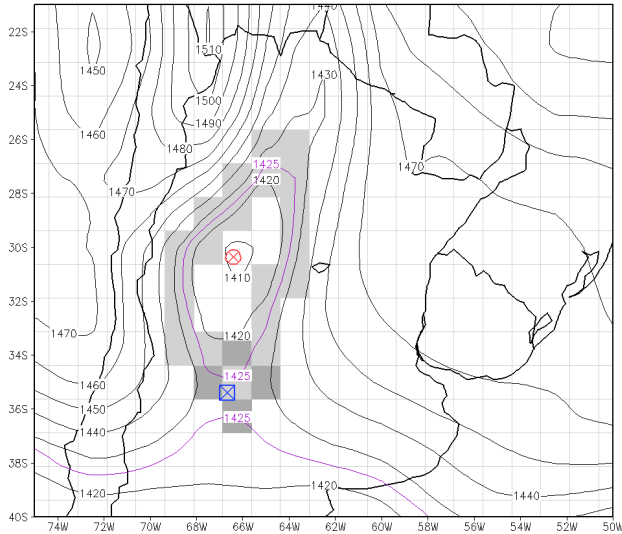


Fig. 4. Testing if NAL is inside the contour level that goes through AC. The contours show ϕ_{850} (m) with the tested contour in purple. The grid-boxes crossed by this contour are highlighted and ACs position is given by the blue box.

the geopotential field, there must be a equigeopotential line which goes through the AC and around the NAL.

Firstly the algorithm follows the equigeopotential leaving each of the saddle points. For each of these lines that formed a closed loop, the algorithm then verifies if it embraces the NAL. This is shown in Fig. 4. If it does, i.e., if AC and LPT were found, all information gathered for the NAL, AC and LPT structures are recorded and the algorithm advances in time and processes the next 6 h field.

3 Results

We applied our algorithm to data described in Sect. 2 and the AC was detected in 42% of the 10 184 time instants analyzed. Its occurrence is highly spatially concentrated in the region of maximum climatological frontogenesis by deformation in equivalent potential temperature (Arraut, 2007), as shown by a comparison of the top and lower panels in Fig. 5. For this reason, it was interesting to investigate the role of the Argentinean Col for frontogenesis in a statistical point of view. The region R, 30°–42.5° S and 62.5°–70° W, was defined for this statistical study (black rectangle in Fig. 5). It contains the region of maximum occurrence of the AC and allows some room so that frontogenesis occurring near the col can be taken into account. The average of the positive values of frontogenesis over R (DFG3+) was defined and calculated as in Arraut and Barbosa (2009) for all 10 184 time instants. Similarly, DFG3– was defined as the average of the negative values of frontogenesis.

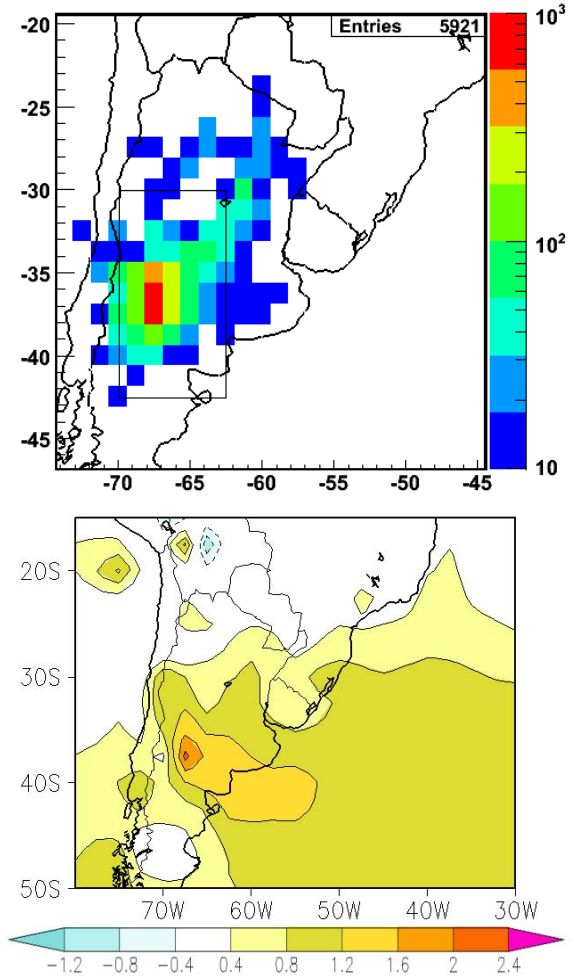


Fig. 5. Top: 2-D-Histogram of the occurrences of the AC with the LPT detected by our algorithm in the studied period. The number of events in each grid box is shown in a color-log scale. Lower: climatology of frontogenesis by deformation in equivalent potential temperature at 850 hPa. Color scale is in K/100 km/day.

Figure 6 shows the distribution of DFG3+ for all time instants analyzed (black), and also separately for the cases when the AC was detected (red) and when the AC was not detected (blue). The AC curve is shifted towards higher values of frontogenesis when compared to the no-AC curve. The first one is centered approximately around DFG3+=1.5 K/100 km/day whereas the second one is centered around 0.8 K/100 km/day. Mean, median and mode are larger for the situations when the AC and LPT are present, showing statement (a): the AC and LPT favor frontogenesis.

Although the total number of no-AC cases is larger than the total number of AC ones, the histograms intersect and AC cases become more numerous above a threshold of DFG3+=1.8 K/100 km/day. The AC histogram exhibits a heavier tale. This can be more clearly seen in the lower panel

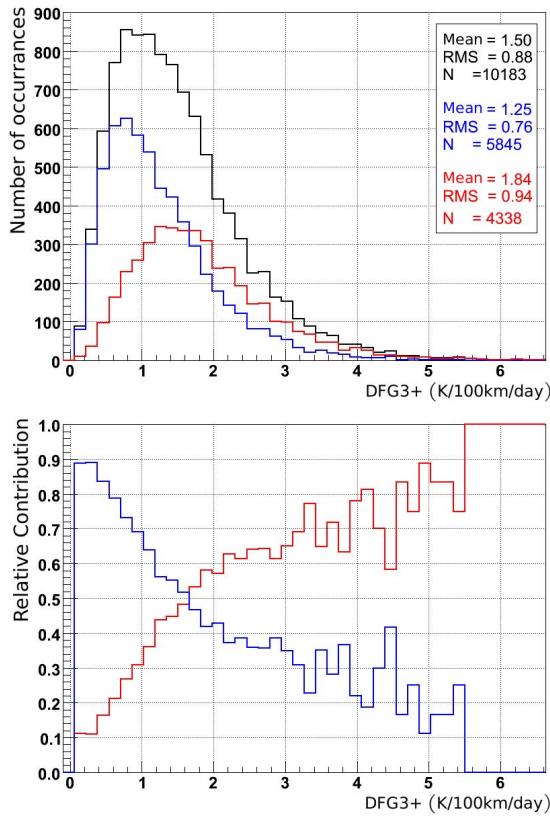


Fig. 6. Top: Histograms showing the distribution of DFG3+ for: all the time instants (black), only those when the AC was detected (red), and only those when the AC was not detected (blue). Lower: the relative contribution of the cases with (red) and without AC (blue).

of Fig. 6 which shows the relative distributions of DFG3+ for AC and no-AC cases. In other words, for each value of DFG3+ the curves show the fractions of AC and no-AC events relative to the total number of events. The fraction of AC cases grows steadily with increasing DFG3+ until about 2.7 K/100 km/day which, as Table 3 shows is the 0.9 quantile. Above this value growth goes on but with more noise since the number of events is small. This shows statement (b): the higher the frontogenesis the higher the statistical presence of the AC and LPT.

Table 3 shows values of DFG3+ corresponding to important quantiles as well as the AC fraction for events above and below these quantiles. Above the 0.5 quantile the AC fraction is around 57%. This grows to almost 70% for events above the 0.9 quantile and over 86% for events above the 0.995 quantile, which are slightly over 50 in number. The AC fraction is well above 50% for all quantiles above 0.5, which shows statement (c): the AC and LPT are present in the majority of events of high frontogenesis.

Table 1. DFG3+ quantiles and the fraction of events in which the AC is present in R for the events with DFG3+ above or lower than the quantile value.

Quantile q	Value of DFG3+	Fraction with Argentinean Col DFG3+ > q	DFG3+ < q
0.25	0.85	50.1%	20.0%
0.50	1.34	57.1%	28.0%
0.75	1.95	64.0%	35.3%
0.90	2.70	68.2%	39.7%
0.95	3.18	73.4%	41.0%
0.99	4.35	78.4%	42.2%
0.995	4.85	86.3%	42.4%

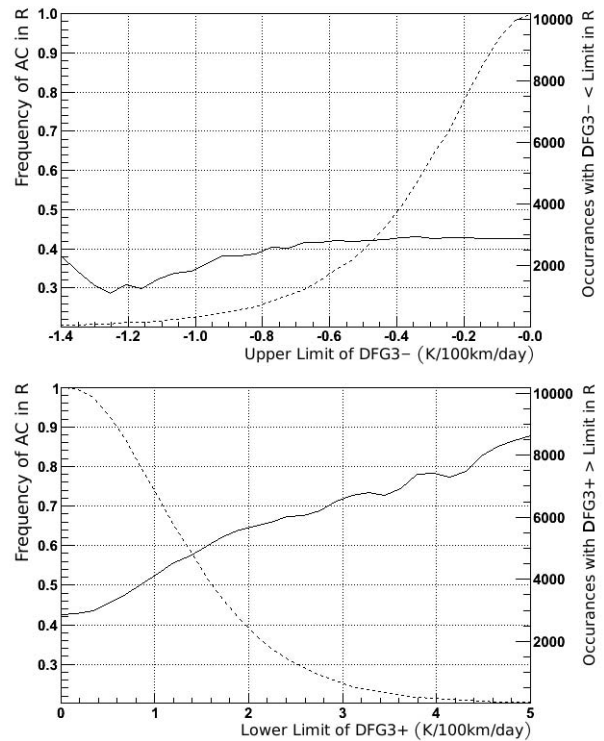


Fig. 7. Right: horizontal axis represents limiting values of DFG3+. The dashed line curve shows the number of events with DFG3+ greater than limit, while the continuous line curve shows the fraction of these events in which AC was found in R. Left: same as the right panel but for DFG3- lower than limit.

In the lower panel of Fig. 7 the dotted curve takes values in the right vertical axis and shows the total number of events above the DFG3+ thresholds shown on the x-axis. The full line curve take values in the left vertical axis and shows the AC fraction for events above the threshold. It is an expanded version of the information in the three columns on the left of Table 3. It shows how the AC fraction steadily grows as DFG3+ thresholds increases.

The plots shown in the upper panel of Fig. 7 are analogous to those in the lower panel, but they refer to negative frontogenesis, or frontolysis. The dotted curve shows the total number of events below the DFG3– threshold. Frontolysis is weaker when compared to frontogenesis. The first reaches values of -1.5 K/100 km/day while the latter reaches values up to $+5$ K/100 km/day. It can also be seen that the intensity of frontolysis shows no appreciable correlation with the presence of the AC and LPT.

4 Conclusions

A quantitative evaluation of the importance of the Argentinean Col and the Low Pressure Tongue east of the Andes for frontogenesis by deformation in the South American subtropics was presented in this paper. It was shown that:

- (a) the presence of the AC and LPT favors frontogenesis,
- (b) the higher the frontogenesis the higher the statistical presence of these features,
- (c) the AC and LPT are present in the majority of cases of high frontogenesis.

Based on these results it can be concluded that the AC and LPT represent the single most important synoptic situation associated with high frontogenesis in the South American subtropics. Even though these are local features of the pressure field, this statement does not diminish the role of transient disturbances, which are an important cause of the strengthening of the NAL (Lichtenstein, 1980; Seluchi et al., 2003; Ferreira, 2008). In fact, in Arraut and Barbosa (2009) it is shown that *strong* frontogenesis is linked to *strong* NAL and LPT events with a baroclinic trough south of the AC and a maximum of wind speed in high levels. It is also shown that these events tend to be associated with strong convective rainfall. It is therefore the *interaction* between transient disturbances and local pressure field features of the South American subtropics that make it so prone to frontogenesis in equivalent potential temperature and strong convection.

Since we cannot distinguish cause and effect with the statistical approach used to quantify the importance of AC and LPT for frontogenesis, one could ask whether the inverse relation holds, i.e., could frontogenesis promote the formation of AC and LPT? To clarify this issue it is important to note that the AC is a geometrical necessity whenever the NAL is formed. This can be easily seen by considering the geostrophic wind. A col is necessary to separate the easterlies south of the NAL from the extra-tropical westerlies.

While the idea of frontogenesis by deformation being favored in the neighborhood of a col, first put forward by Pettersen (1956), is quite simple, a *direct* manner in which frontogenesis may locally promote col formation is hard to imagine. However, an *indirect* mechanism for this, in South

America, has been proposed (Arraut, 2007): frontogenesis intensifies and/or maintains a high level jet, perpetuating the Zonda wind adiabatic forcing and hence the NAL and AC.

An interesting issue for future studies is whether the NAL and LPT formation are more predictable than frontogenesis itself, in which case topic forecasting or nowcasting the LPT could be useful for weather prediction.

Acknowledgements. This research was partially financed by “Coordenadoria de Aperfeiçoamento de Pessoal do Ensino Superior (CAPES)”. ECMWF ERA40 data used in this study have been obtained from the ECMWF data server.

Edited by: R. Garraud

Reviewed by: two anonymous referees

References

- Acton, F. S.: Numerical methods that work, Mathematical Association of America, Washington, corrected edition edn., 1990.
- Arraut, J. M.: Fronts and frontogenesis during summer: geometrical and dynamical aspects and the influence over rainfall on the South American subtropics, Ph.D. thesis, Centro de Previsão de Tempo e Estudos Climáticos – INPE, Rodovia Presidente Dutra Km 40 Cachoeira Paulista, São Paulo, Brasil, online available at: <http://urlib.net/sid.inpe.br/mtc-m17@80/2007/12.19.10.53>, 2007 (in Portuguese).
- Arraut, J. M. and Barbosa, H. J. M.: Large Scale Features Associated with Strong Frontogenesis in Equivalent Potential Temperature in the South American Subtropics East of the Andes, *Adv. Geo.*, this special volume, 2009.
- Bolton, D.: The Computation of Equivalent Potential Temperature, *Mon. Weather Rev.*, 108, 1046–1053, 1980.
- Ferreira, L.: Causes and Variability of the Northwestern Argentinean Low and Impacts Over Local Circulation Patterns, Ph.D. thesis, Universidade de Buenos Aires, 2008 (in Spanish).
- Kodama, Y.-M.: Large-Scale Common Features of Subtropical Precipitation Zones (the Baiu Frontal Zone, the SPCZ and the SACZ) Part I: Characteristics of Subtropical Frontal Zones, *J. Meteorol. Soc. Jpn.*, 70, 813–835, 1992.
- Lichtenstein, E. R.: La depresion del noroeste argentino (The northwestern Argentinian low), Ph.D. thesis, Departamento de Ciencias de la Atmosfera, Ciudad Universitaria (1428) Buenos Aires, Argentina, 1980.
- Ninomiya, K.: Characteristics of Baiu Front as a predominant subtropical front in the summer northern hemisphere, *J. Meteorol. Soc. Jpn.*, 62, 880–894, 1984.
- Pettersen, S.: Weather analysis and forecasting, McGraw-Hill, New York, 2nd edn., 1956.
- Press, W. H., Flannery, B. P., Teukolsky, S. A., and Vetterling, W. T.: Numerical recipes in Fortran 77: the art of scientific computing, Cambridge University Press, Cambridge, 2 edn., 1992.
- Seluchi, M. E., Saulo, C., Nicolini, M., and Satyamurty, P.: The Northwestern Argentinean Low: A study of two typical events, *Mon. Weather Rev.*, 132, 2361–2378, 2003.